



# Density functional theory studies on pyrolysis mechanism of $\beta$ -O-4 type lignin dimer model compound

Jinbao Huang<sup>a,\*</sup>, Chao Liu<sup>b</sup>, Dan Wu<sup>c</sup>, Hong Tong<sup>a,\*</sup>, Lirong Ren<sup>a</sup>

<sup>a</sup> School of Science, Guizhou Minzu University, Guiyang 550025, China

<sup>b</sup> Key Laboratory of Low-grade Energy Utilization Technologies and Systems, Ministry of Education of China, Chongqing University, Chongqing 400044, China

<sup>c</sup> School of Chemistry and Environmental Science, Guizhou Minzu University, Guiyang 550025, China

## ARTICLE INFO

### Article history:

Received 27 February 2014

Accepted 17 July 2014

Available online 25 July 2014

### Keywords:

Lignin

$\beta$ -O-4 type lignin dimer model compound

Pyrolysis mechanism

Density functional theory

## ABSTRACT

Lignin is the main component of biomass with a complex, heterogeneous, three-dimensional polymeric structure of three main monolignols (*p*-coumaryl, coniferyl, and sinapyl alcohol). In order to understand the pyrolysis mechanism of lignin and identify the chemical pathways for the formations of key products during pyrolysis, the pyrolysis processes of  $\beta$ -O-4 type lignin dimer model compound 1 (1-phenyl-2-phenoxy-1,3-propanediol) were theoretically investigated by employing density functional theory (DFT) methods at the B3LYP/6-31G(d,p) level. Based on related experimental and calculation results of bond dissociation energies of  $\beta$ -O-4 type lignin dimer, three possible pyrolytic pathways (the homolytic cleavage of C $\beta$ –O bond, the homolytic cleavage of C $\alpha$ –C $\beta$  bond and the concerted reactions) were proposed, the activation energies of each reaction step were calculated, and the temperature effect on pyrolysis processes was analyzed. The calculation results indicate that the homolytic cleavage reaction of C $\beta$ –O bond and concerted reaction pathways (3) could be the major reaction channels, and the homolytic cleavage reaction of C $\alpha$ –C $\beta$  bond and concerted reaction pathways (1) and (2) could be the competitive reaction channels in pyrolysis processes. The concerted reactions would dominate over free-radical homolytic reactions at lower temperatures, while at high temperatures the free-radical reaction (C–O homolysis) would dominate over the concerted reactions.

© 2014 Elsevier B.V. All rights reserved.

## 1. Introduction

With increasing concerns about energy supply and environmental pollution problems caused by burning fossil fuels, the utilization of renewable biomass resources has attracted more and more attention. The sulfur, nitrogen and ash contents in biomass are low and biomass energy is a renewable and clean energy, which can reduce the greenhouse effect, making the biomass energy study a hot topic worldwide [1–8]. Biomass liquefaction technology is considered to be the most promising technology in biomass energy utilizing field. Biomass contains varying amounts of cellulose, hemicellulose, lignin and a small amount of extractives [9]. The ratio of the three components in a biomass, which is closely related to biomass conversion, differs greatly along various sources

of biomass [10], the study of the pyrolysis mechanism of biomass components is therefore essential.

Lignin is the second-most abundant naturally occurring biopolymer and a by-product of the pulping process [11]. Pyrolysis of lignin has been studied by some people over the past several decades. Iatridis and Gavalas [12] studied the pyrolysis of a precipitated kraft lignin in a “captive sample” reactor at temperature of 400–700 °C and identified a few compounds by gas chromatography including oxides of carbon, hydrocarbons, methanol, acetone and single-ring phenols (phenol, guaiacol, etc.). Caballero et al. [13] used a semi-batch flow reactor connected in series between a Pyroprobe 1000 and a gas chromatographer to study the production of gases from kraft lignin at different nominal temperatures (ranging from 500 to 900 °C), and analyzed yields of 13 pyrolysis products (methane, ethane, ethylene, propylene, propane, hydrocarbons with four carbon atoms, benzene, other aromatics, CO, CO<sub>2</sub>, methanol together with formaldehyde, acetaldehyde, acetic acid and water). Jiang et al. [14] investigated the temperature dependence of the pyrolysis products of two types of lignin (Alcell lignin and Asian lignin) using PyGC–MS and identified about 50 compounds from lignin pyrolysis

\* Corresponding authors. Tel.: +86 0851 3610156; fax: +86 08513610156.

E-mail addresses: [huangjinbao76@126.com](mailto:huangjinbao76@126.com) (J. Huang), [tonghong63@126.com](mailto:tonghong63@126.com) (H. Tong).

at a temperature range of 400–800 °C. The phenolic compounds yield was 17.2 wt% for Alcell lignin and individual yield of most of the compounds was less than 1 wt%. Wang et al. [15,16] investigated the pyrolysis characteristics of milled wood lignins (MWLs) using a thermogravimetric analyzer, and also analyzed the FTIR profiles of main pyrolysis products (CO<sub>2</sub>, CO, methane, methanol, phenols and formaldehyde).

Lignin model compounds, which have simple structures and product distributions compared to real lignin, have been studied in order to understand the pyrolysis mechanism of lignin. Vuori and Bredenberg [17] studied the thermolyses of *o*-, *m*-, and *p*-hydroxyanisoles under an inert atmosphere, the major products formed from all three hydroxyanisoles were the correspondingly substituted dihydroxybenzenes and cresols, and the reactivity of the lignin-related *o*-hydroxyanisole (guaiacol) was much higher than those of all other model compounds studied. The pyrolysis of phenethyl phenyl ether (PPE) and its methoxy-substituted derivatives were investigated theoretically by Beste et al. [18,19]. They found that the initial step in the thermal decomposition of PPE is the homolytic cleavage of the oxygen–carbon bond, and carbon–carbon bond cleavage in PPE could be a competitive initial reaction under high-temperature pyrolysis conditions. Chu et al. [20] investigated the pyrolysis behavior of a  $\beta$ -O-4 type oligomeric lignin model compound at a temperature range from 250 to 550 °C and proposed a free radical reaction pathway to explain the product chemistry. To obtain information on the thermal reactivities of lignin aromatic nuclei, guaiacyl and syringyl types, thermal reactions of guaiacol (2-methoxyphenol) and syringol (2,6-dimethoxyphenol) were compared in a closed ampoule reactor (N<sub>2</sub>/400–600 °C/40–600 s) by Asmadi et al. [21]. Their experimental results indicated that the O–CH<sub>3</sub> bond homolysis occurring at temperatures higher than 400 °C was the rate-determining step, and the radical induced rearrangement (*ipso*-substitution), demethoxylation and radical coupling reactions to form higher MW products and methylated aromatics were the subsequent reactions.

Lignin is a complex, heterogeneous, three-dimensional polymer and naturally produced by the enzymatic polymerization of three main monolignols (*p*-coumaryl, coniferyl, and sinapyl alcohol), which are interconnected by a variety of linkages ( $\beta$ -O-4,  $\alpha$ -O-4, 4-O-5, 5-5,  $\beta$ -1, etc.). The  $\beta$ -O-4 bond is the major type of linkage which occupies 48–60% of the total linkages depending on the type of wood [22]. Unlike the pyrolysis of cellulose and hemicelluloses [23–25], the complexity of the lignin structure and its high molecular weight present make the lignin pyrolysis more complex, and it is difficult to analyze detailed mechanism through experiments. So people gradually pay more attention to employing theoretical methods to study the pyrolysis mechanism and to forecast possible reaction pathways [26–29]. In order to further improve the understanding of detailed mechanism of lignin pyrolysis and formation mechanism of its main products, the pyrolysis processes of  $\beta$ -O-4 type lignin dimer model compound **1** (1-phenyl-2-phenoxy-1,3-propanediol, shown in Fig. 1) have been theoretically investigated by using density functional theory methods at B3LYP/6-31G(d,p) level in this paper.

## 2. Calculation methods

The geometries of reactant, intermediates, transition states and products have been optimized by employing the hybrid density functional B3LYP (Becke's three parameter gradient corrected exchange functional [30] with the gradient corrected correlation functional of Lee et al. [31]) with the 6-31G(d,p) basis set. Stationary points on the potential energy surface of the reacting system were fully optimized using gradient minimization techniques, followed by evaluating harmonic vibration frequencies to characterize

their nature as minima (all real frequencies) or first-order saddle points (namely transition states, only one imaginary frequency). No constrain in the initial molecular geometry for searching symmetric and asymmetric transition states was used in their optimization procedure. Intrinsic reaction coordinate (IRC) [32] calculations have been performed to identify the minimum energy path from a transition state to the two corresponding local minima. Activation energies (the reaction energy barriers) for reactions were estimated as the relative energies, including zero-point energy correction (ZPE), between the transition state and the reactant. The standard thermodynamic changes were energy differences between the reactants and the products, including the ZPE. For free-radical reactions, the bond dissociation energies may serve as approximations to the activation energies. Gaussian 03 suites of programs were employed for all calculations [33].

## 3. Results and discussion

### 3.1. Bond dissociation energies for $\beta$ -O-4 type lignin dimer model compound

Bond dissociation energies ( $\Delta E$ ) are fundamental to understand many chemical processes because they exemplify the reaction energy of a homolytic cleavage of the considered bond. The homolytic bond dissociation is an important reaction step in lignin pyrolysis. Fig. 1 shows the homolytic cleavage ways of  $\beta$ -O-4 type lignin dimer model compound and their bond dissociation energies calculated at B3LYP/6-31G(d,p) level. The bond dissociation energy of C <sub>$\beta$</sub> –O, 245.3 kJ/mol, is the lowest, and that of C <sub>$\alpha$</sub> –C <sub>$\beta$</sub> , 259.2 kJ/mol, is the second lowest. The order of  $\Delta E$  is as follows: C <sub>$\beta$</sub> –O < C <sub>$\alpha$</sub> –C <sub>$\beta$</sub>  < C <sub>$\alpha$</sub> –OH < C <sub>$\beta$</sub> –C <sub>$\gamma$</sub>  < C<sub>aromatic</sub>–C <sub>$\alpha$</sub>  < C<sub>aromatic</sub>–O, therefore, the initial step in the thermal decomposition of  $\beta$ -O-4 type lignin dimer model compound could be the homolytic cleavage of the C <sub>$\beta$</sub> –O bond, and C <sub>$\alpha$</sub> –C <sub>$\beta$</sub>  bond cleavage could be a competitive initial reaction.

### 3.2. Pyrolysis mechanism of $\beta$ -O-4 type lignin dimer model compound

Lignin pyrolysis experimental results [14,34,35] indicated that the main pyrolysis products were single-ring phenolic compounds, methanol, formaldehyde, acetaldehyde, CO, CH<sub>4</sub>, etc. Britt et al. [22] studied the fast vacuum pyrolysis of methoxy-substituted  $\beta$ -O-4 lignin model compounds and proposed a complex reaction pathway which was dominated by free-radical reactions, molecular rearrangements, and concerted elimination reactions. In this paper, we propose three possible pyrolysis ways: the homolytic cleavage of C <sub>$\beta$</sub> –O bond, the homolytic cleavage of C <sub>$\alpha$</sub> –C <sub>$\beta$</sub>  bond and the concerted reactions.

#### 3.2.1. The homolytic cleavage of C <sub>$\beta$</sub> –O bond

According to the above calculation results of bond dissociation enthalpies of  $\beta$ -O-4 type lignin dimer model compound, the bond dissociation energy of C <sub>$\beta$</sub> –O bond is the lowest, 245.3 kJ/mol, and the homolytic cleavage of C <sub>$\beta$</sub> –O bond is the major pyrolysis way in pyrolysis of lignin. Fig. 2 gives the possible reaction pathways for the homolytic cleavage of C <sub>$\beta$</sub> –O bond, the potential energy profile along reaction pathways is shown in Fig. 3, and the optimized geometries of reactant, intermediates, transition states, and products in pyrolysis processes of the homolytic cleavage of C <sub>$\beta$</sub> –O bond are shown in Fig. 4.

Model compound **1** can decompose into radicals **2** and **3**, then the radical **3** is converted into phenol **4** through hydrogenation reaction, which is exothermic with an energy of –340.3 kJ/mol. Radical **2** can undergo a dehydrogenation to form phenylallyl alcohol **5** via the transition state **T1** with an energy barrier of 143.3 kJ/mol,

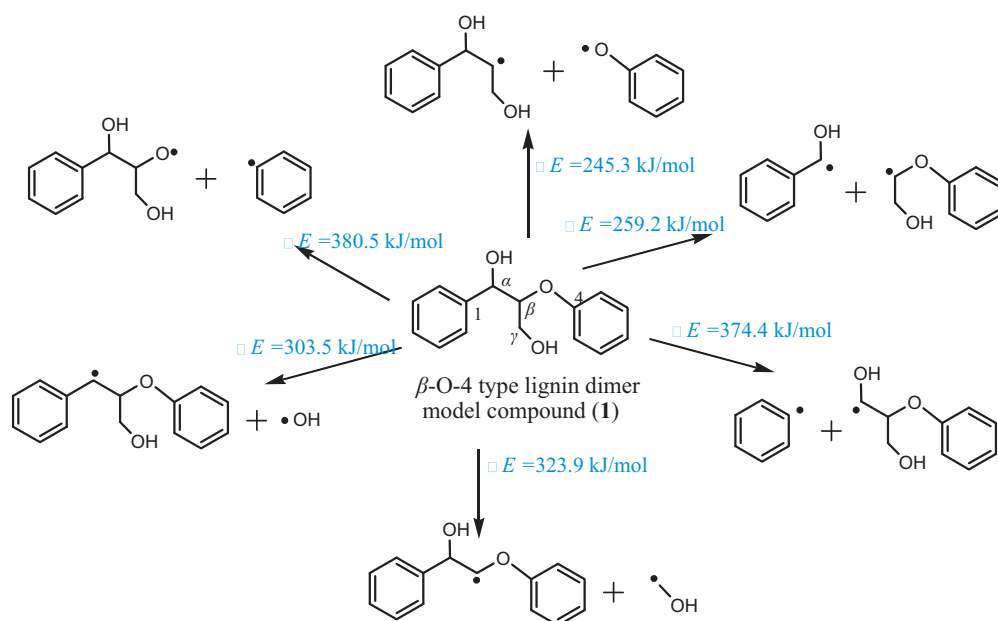


Fig. 1. Homolytic cleavage ways of  $\beta$ -O-4 type lignin dimer model compound and their bond dissociation enthalpies ( $\Delta E$ ).

absorbing an energy of 124.2 kJ/mol, or it can undergo a hydrogenation to form phenyl propanediol **9**, releasing an energy of 378.4 kJ/mol. Compound **5** can tautomerize to form phenyl acetone alcohol **6** via **T2** with an activation energy of 200.1 kJ/mol through

intramolecular hydrogen transfer. The tautomerization reaction is exothermic and compound **6** is more stable than its enol form compound **5**. Compound **6** can decompose into acetophenone **7** and formaldehyde via transition state **T3** with an energy barrier

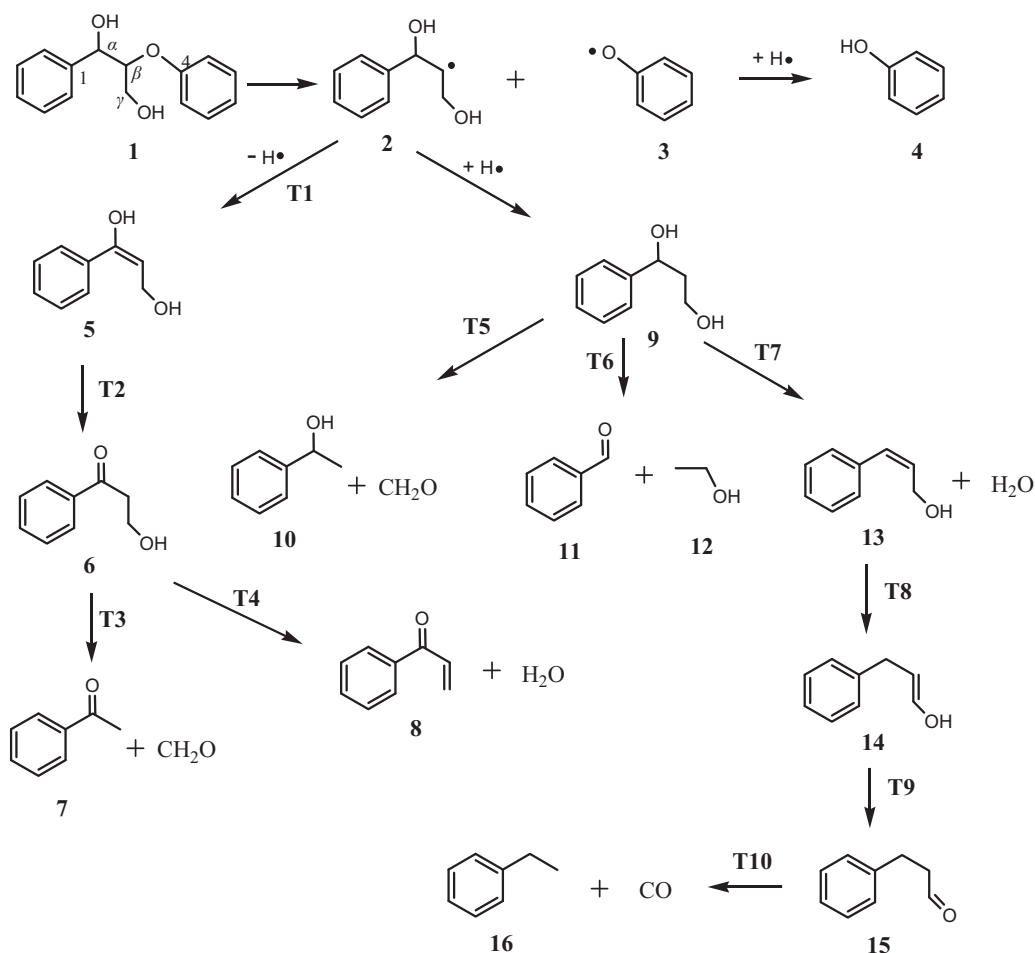


Fig. 2. The proposed reaction pathways in pyrolysis processes of the homolytic cleavage of  $C_{\beta}$ -O bond.

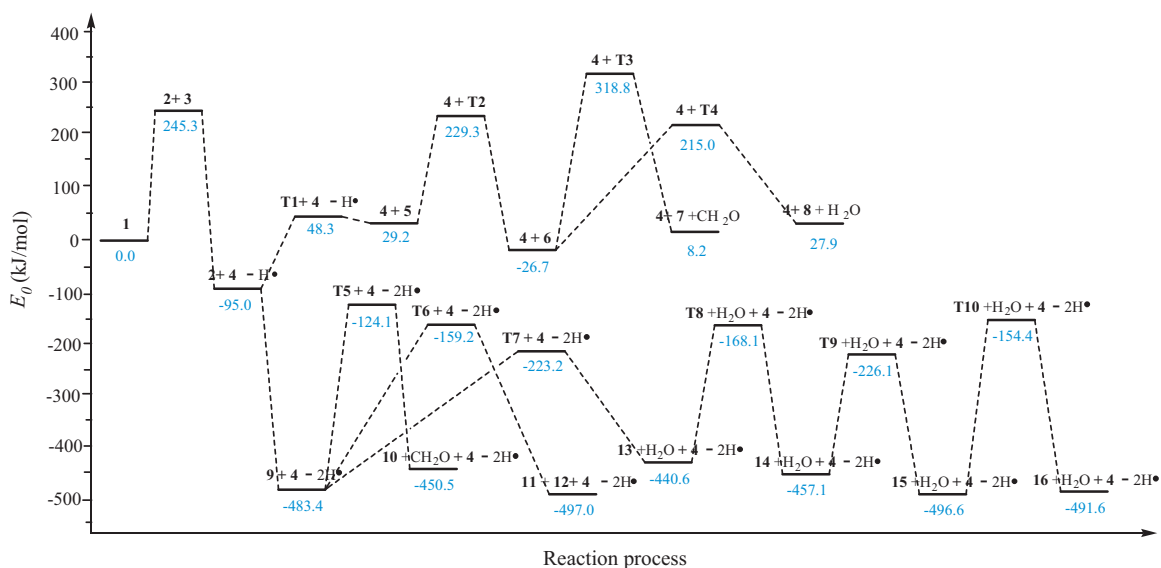


Fig. 3. Potential energy profile along reaction pathways in pyrolysis processes of the homolytic cleavage of  $C_{\beta}$ –O bond.

of 345.5 kJ/mol, or it can undergo a dehydration reaction to form phenyl acrylketone **8** and  $H_2O$  via transition state **T4** with an energy barrier of 241.7 kJ/mol. Phenyl propanediol **9** can decompose via three pathways. In pathway (1), compound **9** decomposes to form phenethyl alcohol **10** and formaldehyde via transition state **T5** with an energy barrier of 359.3 kJ/mol. In pathway (2), compound **9** decomposes to form benzaldehyde **11** and ethyl alcohol **12** via transition state **T6** with an energy barrier of 324.2 kJ/mol. In pathway (3), compound **9** undergoes a dehydration reaction to form compound **13** and  $H_2O$  via transition state **T7** with an energy barrier of 260.2 kJ/mol, and compound **13** tautomerizes to form compound **14** via **T8** with an energy barrier of 272.5 kJ/mol through intramolecular hydrogen transfer. From the optimized structure of **T8** in Fig. 4, there is a transfer of hydrogen atom from  $C_{\gamma}$  to  $C_{\alpha}$ , meanwhile  $C_{\alpha}$ – $C_{\beta}$  double bond lengthens to transform into single bond and  $C_{\beta}$ – $C_{\gamma}$  bond shortens to transform into double bond. Compound **14** can further tautomerize to form benzenepropanal **15** via **T9** with an activation energy of 231.0 kJ/mol. Benzenepropanal **15** can decarbonylate to form phenylethane **16** and CO via **T10** with an energy barrier of 342.2 kJ/mol.

Through comparisons of energy barriers of each reaction step in pyrolysis processes of the homolytic cleavage of  $C_{\beta}$ –O bond, we would infer that the major products of model compound **1** pyrolysis appear to be phenol **4**, phenyl acetone alcohol **6**, phenyl acrylketone **8**, phenyl propanediol **9**, benzenepropanal **15**, etc.

### 3.2.2. The homolytic cleavage of $C_{\alpha}$ – $C_{\beta}$ bond

Fig. 5 gives the possible reaction pathways for the homolytic cleavage of  $C_{\alpha}$ – $C_{\beta}$  bond, the potential energy profile along reaction pathways is shown in Fig. 6, and the optimized geometries of reactants, intermediates, transition states, and products in pyrolysis processes of the homolytic cleavage of  $C_{\alpha}$ – $C_{\beta}$  bond are shown in Fig. 7. The radicals **17** and **18** can be formed through the homolytic cleavage of the  $C_{\alpha}$ – $C_{\beta}$  bond. The radical **18** can be converted into phenylcarbinol **19** through hydrogenation reaction, releasing an energy of 332.5 kJ/mol, or into benzaldehyde **11** through dehydrogenation reaction via transition state **T11** with an energy barrier of 157.6 kJ/mol. The radical **17** can decompose through three pathways. In pathway (1), radical **17** loses a hydrogen atom through  $\beta$ -scission to form phenoxy vinyl alcohol **25** via transition state **T12** with an energy barrier of 217.6 kJ/mol. Phenoxy vinyl alcohol **25** tautomerizes to form phenoxy acetaldehyde **28** via **T13** with

an energy barrier of 225.9 kJ/mol through intramolecular hydrogen shift. Phenoxy acetaldehyde **28** may decarbonylate to produce anisole **21** via **T14** with a high energy barrier of 340.6 kJ/mol. In pathway (2), radical **17** decomposes to form radical **24** and formaldehyde via **T15** with a low energy barrier of 83.7 kJ/mol. Radical **24** tautomerizes to form radical **26** via **T16** with an energy barrier of 86.2 kJ/mol, then the radical **26** is further converted into radical **27** through the cleavage of the C–O bond and releases an energy of 51.1 kJ/mol. The radical **27** can pick up a hydrogen atom to become phenylcarbinol **19**, releasing an energy of 404.2 kJ/mol, or it can lose a hydrogen atom to form benzaldehyde **11** via transition state **T17** with a low energy barrier of 80.9 kJ/mol. In pathway (3), radical **17** undergoes a hydrogenation to form phenoxy alcohol **20**, releasing an energy of 383.1 kJ/mol. Phenoxy alcohol **20** may decompose to form anisole **21** and formaldehyde via **T18** with a high energy barrier of 367.7 kJ/mol, or it may form phenol **4** and vinyl alcohol **22** via **T19** with an energy barrier of 257.1 kJ/mol, which is similar to a dehydration reaction. From the optimized structure of **T19** in Fig. 7,  $C_{\beta}$ –O and  $C_{\gamma}$ –H bonds rupture, meanwhile  $C_{\beta}$ – $C_{\gamma}$  bond shortens to transform into double bond. Vinyl alcohol **22** can tautomerize to form acetaldehyde **23** via **T20** with an energy barrier of 224.0 kJ/mol through intramolecular hydrogen transfer and release an energy of 50.8 kJ/mol.

Through comparisons of energy barriers of each reaction step in pyrolysis processes of the homolytic cleavage of  $C_{\alpha}$ – $C_{\beta}$  bond, we would infer that the major products of model compound **1** pyrolysis appear to be phenol **4**, benzaldehyde **11**, phenylcarbinol **19**, phenoxy alcohol **20**, acetaldehyde **23**, phenoxy acetaldehyde **28**, etc.

### 3.2.3. The concerted reactions

Fig. 8 gives four possible concerted reaction pathways in pyrolysis processes of  $\beta$ -O-4 type lignin dimer model compound, the potential energy profile along reaction pathways is shown in Fig. 9, and the optimized geometries of reactant, intermediates, transition states, and products in concerted reaction pathways are shown in Fig. 10. In concerted reaction pathway (1), model compound **1** decomposes directly to form phenol **4** and intermediate **29** via transition state **T21** with an energy barrier of 257.1 kJ/mol through concerted elimination reaction without the intermediacy of free radicals. From the optimized structure of **T21** in Fig. 10, bond  $C_{\beta}$ –O and bond O–H on  $C_{\alpha}$  rupture, meanwhile phenol **4** is formed.



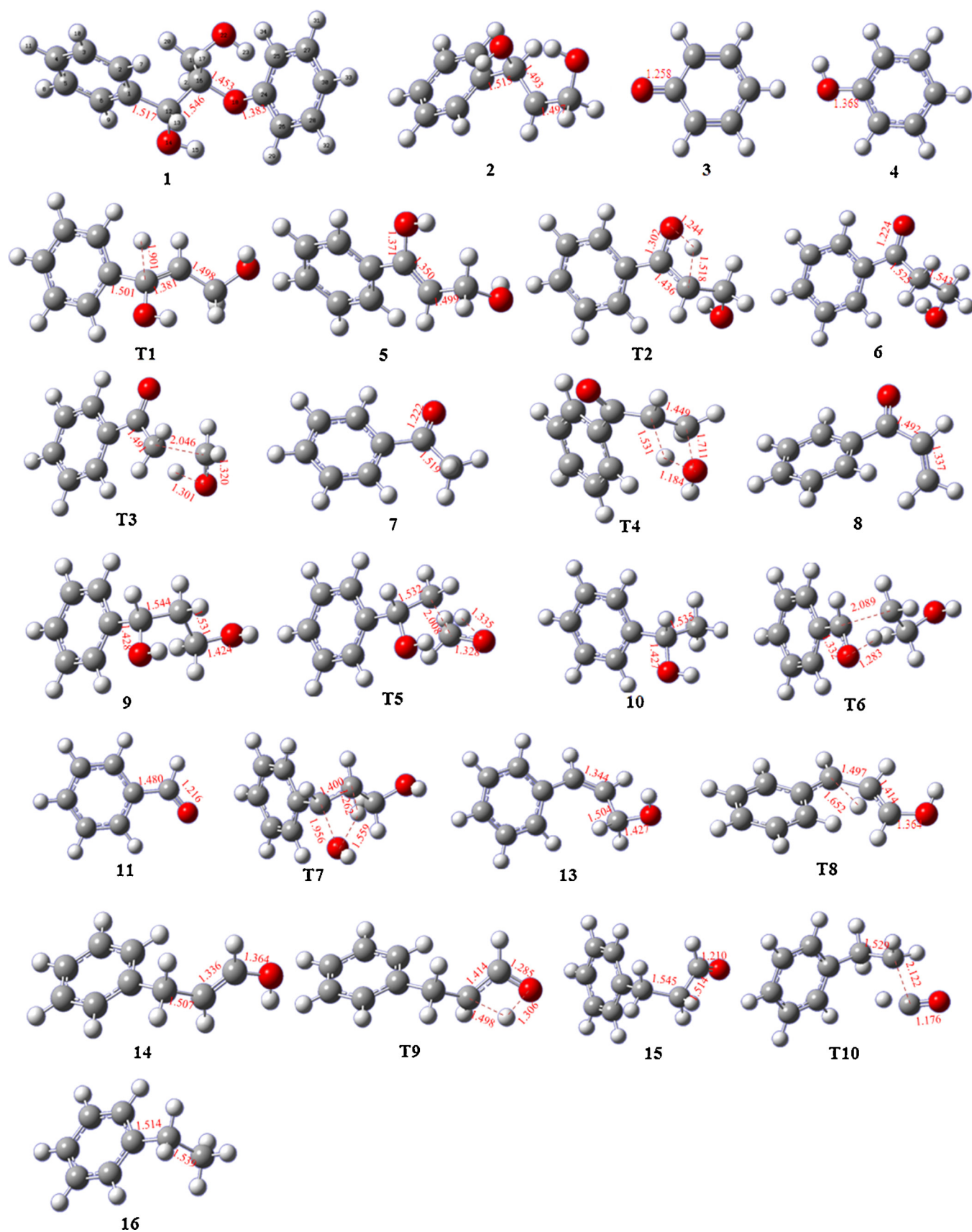


Fig. 4. Optimized geometries of reactant, intermediates, transition states, and products in pyrolysis processes of the homolytic cleavage of  $C_\beta-O$  bond (unit: Å).

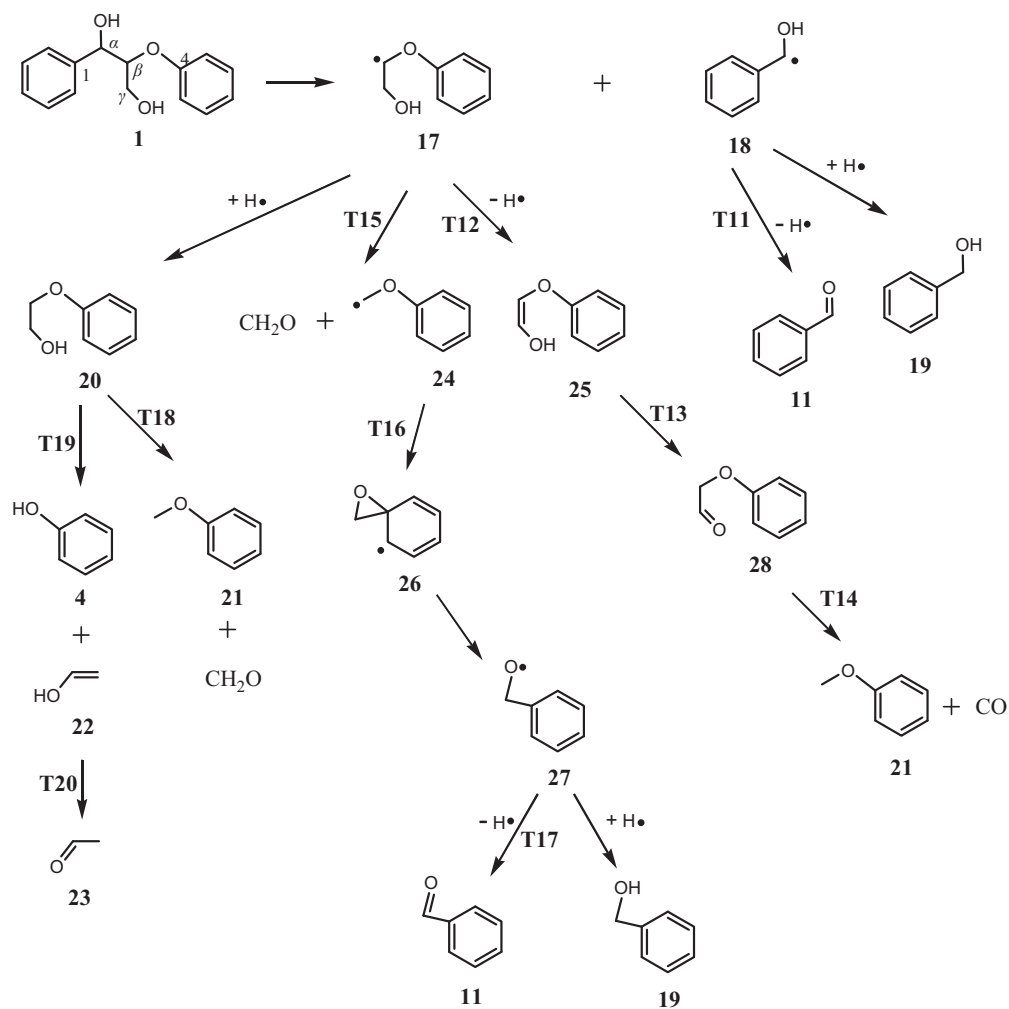


Fig. 5. The proposed reaction pathways in pyrolysis processes of the homolytic cleavage of  $C_\alpha-C_\beta$  bond.

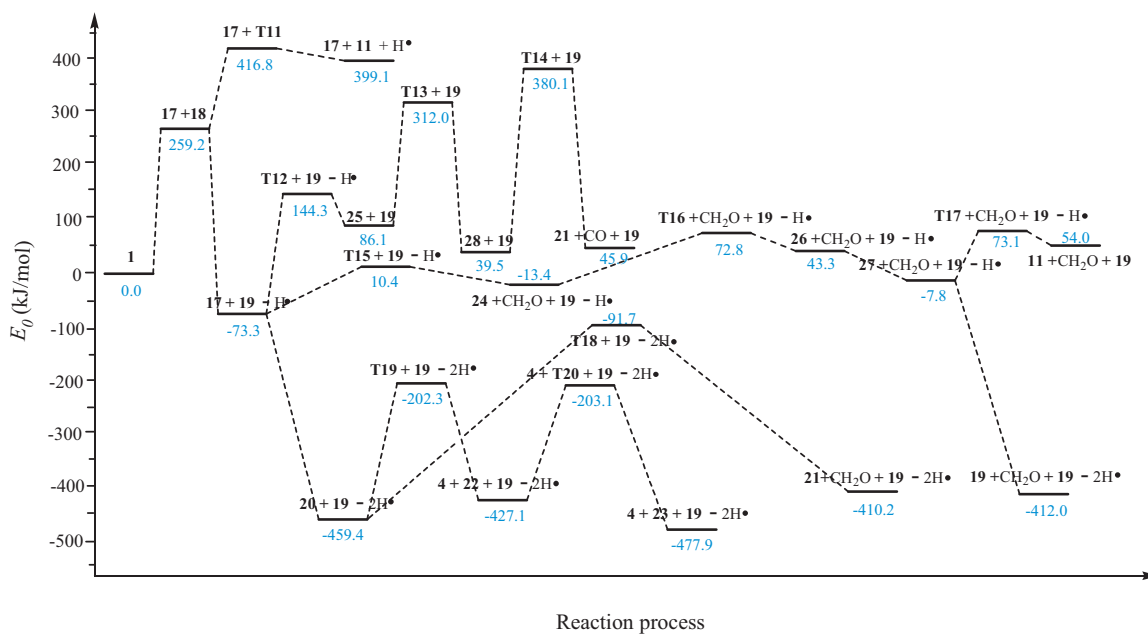


Fig. 6. Potential energy profile along reaction pathways in pyrolysis processes of the homolytic cleavage of  $C_\alpha-C_\beta$  bond.

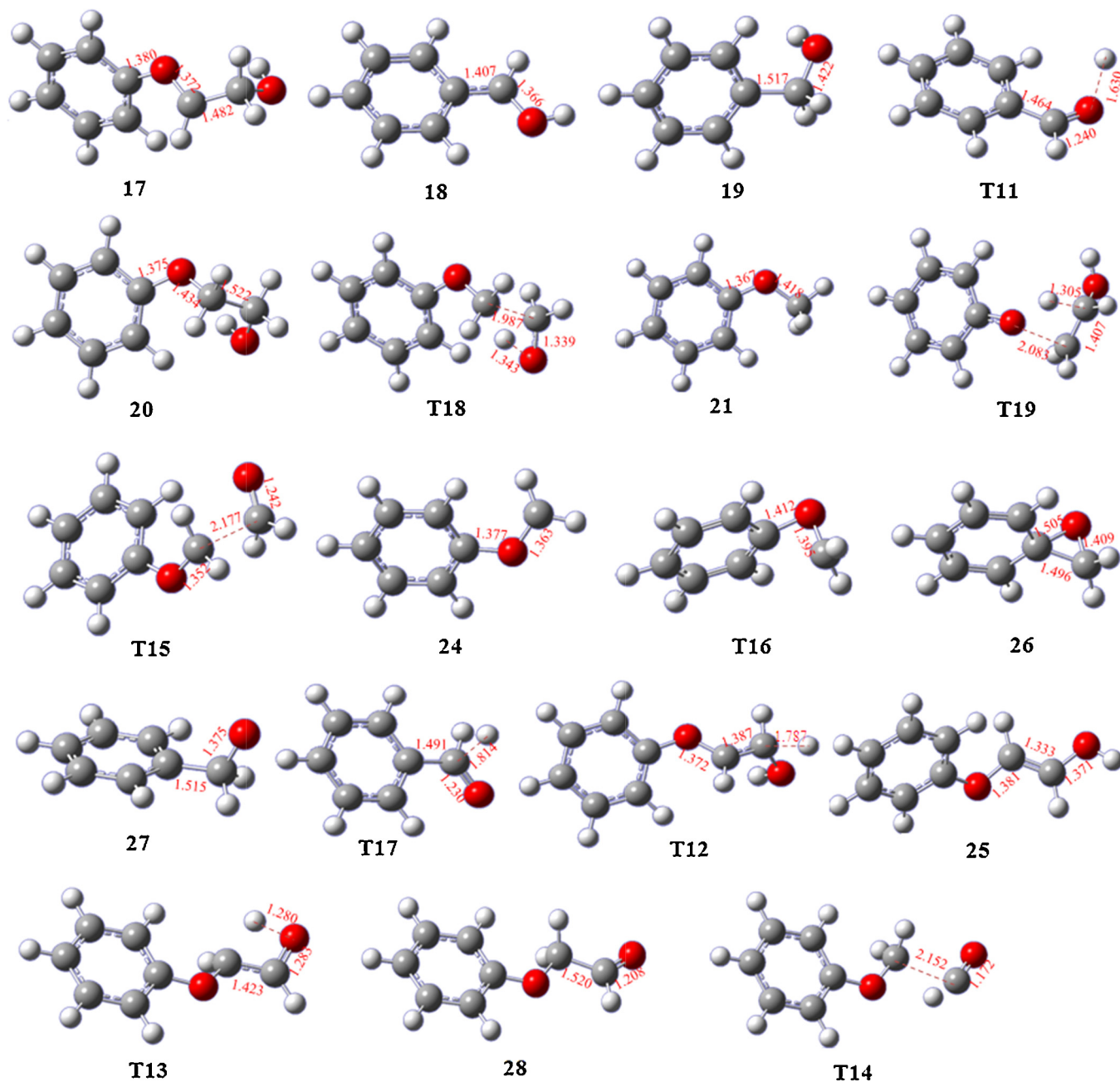


Fig. 7. Optimized geometries of reactant, intermediates, transition states, and products in pyrolysis processes of the homolytic cleavage of  $C_{\alpha}-C_{\beta}$  bond (unit: Å).

Intermediate **29** tautomerizes to form phenyl acetone alcohol **6** via **T25** with an energy barrier of 258.1 kJ/mol through intramolecular hydrogen transfer, releasing an energy of 111.6 kJ/mol. From the optimized structure of **T25** in Fig. 10, there is a transfer of hydrogen atom from  $C_{\alpha}$  to  $C_{\beta}$ , meanwhile  $O-C_{\beta}$  bond ruptures and  $O-C_{\alpha}$  bond shortens to transform into double bond. Compound **6** may further decompose into acetophenone **7** and formaldehyde via transition state **T3** with a high energy barrier of 345.5 kJ/mol. In concerted reaction pathway (2), phenol **4** and 3-hydroxy-3-phenyl-propaldehyde **30** are directly formed via transition state **T22** with an energy barrier of 240.1 kJ/mol through concerted elimination reaction without the intermediacy of free radicals. It can be seen from the optimized structure of **T22** in Fig. 10 that  $C_{\beta}-O$  bond and  $O-H$  bond on  $C_{\gamma}$  rupture, meanwhile  $O-C_{\gamma}$  bond shortens to transform into double bond and phenol **4** is formed. 3-hydroxy-3-phenyl-propaldehyde **30** may decarbonylate to form

phenethyl alcohol **10** and CO via **T26** with a high activation energy of 335.0 kJ/mol, and phenethyl alcohol **10** may undergo a demethylation to form benzaldehyde **11** and  $CH_4$  via transition state **T27** with an energy barrier of 325.8 kJ/mol through concerted elimination reaction. In concerted reaction pathway (3), model compound **1** decomposes directly to form phenol **4** and phenylallyl alcohol **5** via transition state **T23** with an energy barrier of 219.3 kJ/mol. It can be seen from the optimized structure of **T23** in Fig. 10 that  $C_{\beta}-O$  bond and  $O-H$  bond on  $C_{\alpha}$  rupture, meanwhile  $C_{\alpha}-C_{\beta}$  bond has been shortened from 1.546 Å to 1.421 Å to transform into double bond and phenol **4** and phenylallyl alcohol **5** are formed. Phenylallyl alcohol **5** can tautomerize to form phenyl acetone alcohol **6** via **T2** with an activation energy of 200.1 kJ/mol through intramolecular hydrogen transfer, releasing an energy of 55.9 kJ/mol. Phenyl acetone alcohol **6** may further decompose into acetophenone **7** and formaldehyde. In concerted reaction pathway (4), benzaldehyde





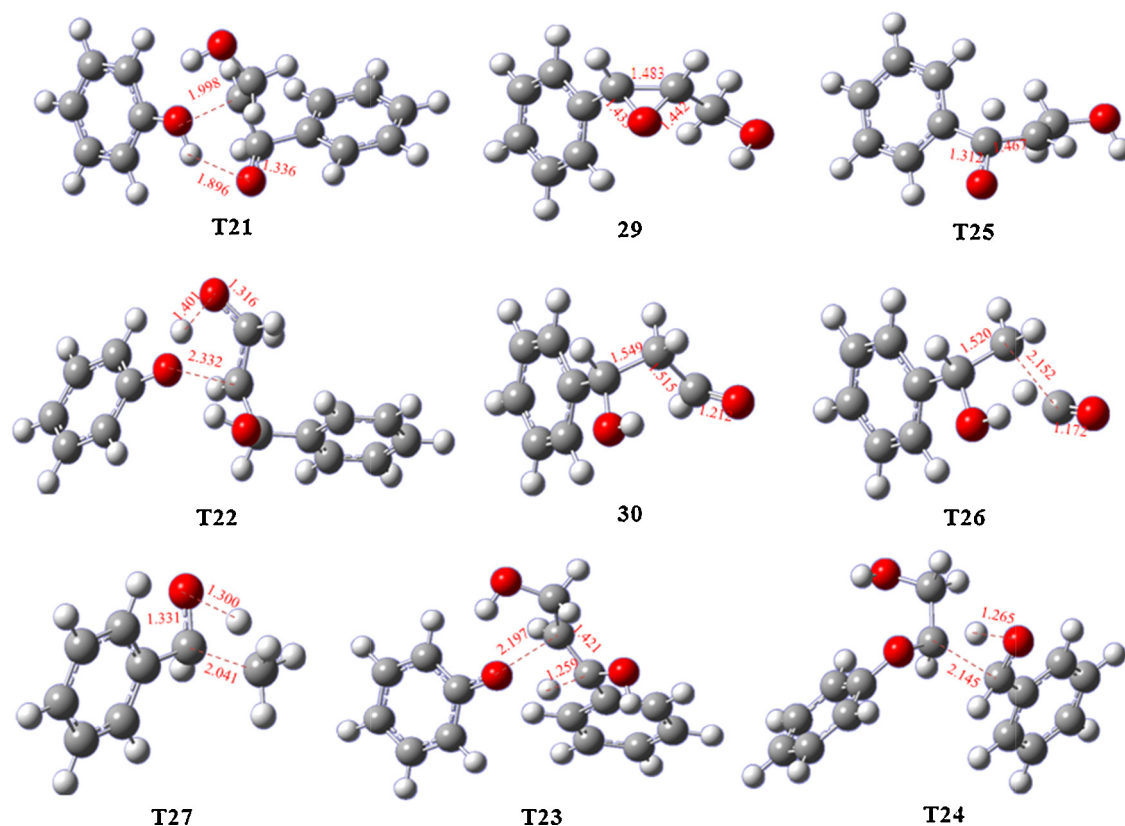


Fig. 10. Optimized geometries of reactant, intermediates, transition states, and products in four concerted reaction pathways (unit: Å).

**11** and phenoxy alcohol **20** are directly formed via transition state **T24** with a high energy barrier of 343.9 kJ/mol through concerted elimination reaction. It can be seen from the optimized structure of **T24** in Fig. 10 that  $C_{\alpha}-C_{\beta}$  bond and O–H bond on  $C_{\alpha}$  rupture, meanwhile O– $C_{\alpha}$  bond shortens to transform into double bond. Phenoxy alcohol **20** may further decompose through the proposed reaction pathways in Fig. 5.

Comparing energy barriers of initial reaction steps in four possible concerted reaction pathways, it is easy to know that energy barriers of initial reaction steps of concerted reaction pathways (1), (2) and (3) are obviously lower than that of concerted reaction pathway (4), so concerted reaction pathways (1), (2) and (3) are kinetically favorable, and concerted reaction pathway (4) is unlikely to occur in pyrolysis processes of  $\beta$ -O-4 type lignin dimer model compound. For concerted reaction pathways (1), (2) and (3), the energy barrier of initial reaction step of concerted reaction pathway (3) is lower than those of concerted reaction pathways (1) and (2), consequently concerted reaction pathway (3) could be the major reaction channel and concerted reaction pathways (1) and (2) could be the competitive reaction channels in pyrolysis processes of model compound **1**.

Through comparisons of energy barriers of initial reaction steps in three possible pyrolysis ways: the homolytic cleavage reaction of  $C_{\beta}-O$  bond, the homolytic cleavage reaction of  $C_{\alpha}-C_{\beta}$  bond and the concerted reactions, it can be seen that the homolytic cleavage reaction of  $C_{\beta}-O$  bond and concerted reaction pathways (3) could be the major reaction channels, and the homolytic cleavage reaction of  $C_{\alpha}-C_{\beta}$  bond and concerted reaction pathways (1) and (2) could be the competitive reaction channels in pyrolysis processes of  $\beta$ -O-4 type lignin dimer model compound **1**. Hence, the main products of model compound **1** pyrolysis could be phenolic compounds such as phenol **4**, phenyl acetone alcohol **6**, phenyl acrylketone **8**, phenyl propanediol **9** and benzenepropanal **15**, and

the main competitive products could be benzaldehyde **11**, phenylcarbinol **19**, phenyl ether such as phenoxy alcohol **20**, phenoxy vinyl alcohol **25** and phenoxy acetaldehyde **28**. The above analysis results are in accordance with the related experimental results [14,34,35].

### 3.3. Temperature effect on pyrolysis processes of $\beta$ -O-4 type lignin dimer model compound

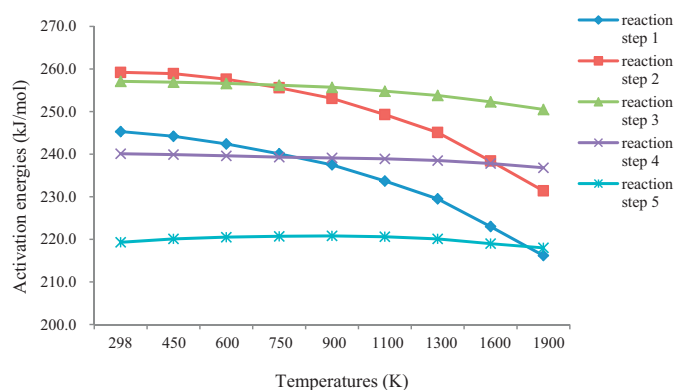
In order to understand the temperature effect on pyrolysis processes of  $\beta$ -O-4 type lignin dimer model compound **1**, activation energies of initial reaction steps in pyrolysis processes of model compound **1** at different temperatures (298, 450, 600, 750, 900, 1100, 1300, 1600, 1900 K) were calculated at B3LYP/6-31G(d,p) level. Table 1 summarizes the activation energies of initial reaction steps at different temperatures, and the relationship between

Table 1

Activation energies of initial reaction steps in pyrolysis processes of model compound **1** at different temperatures.

Temperature (K)	Activation energies (kJ/mol)				
	Reaction step 1	Reaction step 2	Reaction step 3	Reaction step 4	Reaction step 5
298	245.3	259.2	257.1	240.1	219.3
450	244.2	258.9	256.9	239.9	220.1
600	242.4	257.6	256.6	239.6	220.5
750	240.1	255.6	256.2	239.3	220.7
900	237.5	253.1	255.7	239.1	220.8
1100	233.7	249.3	254.8	238.9	220.6
1300	229.5	245.1	253.8	238.5	220.1
1600	223.0	238.4	252.3	237.8	219.0
1900	216.2	231.4	250.5	236.8	218.0

Reaction step 1: **1**  $\rightarrow$  **2** + **3**; reaction step 2: **1**  $\rightarrow$  **17** + **18**; reaction step 3: **1**  $\rightarrow$  **T21**; reaction step 4: **1**  $\rightarrow$  **T22**; reaction step 5: **1**  $\rightarrow$  **T23**.



**Fig. 11.** Relationship between activation energies of initial reaction steps in pyrolysis processes of model compound **1** and temperature (reaction step 1: **1** → **2** + **3**; reaction step 2: **1** → **17** + **18**; reaction step 3: **1** → **T21**; reaction step 4: **1** → **T22**; reaction step 5: **1** → **T23**).

activation energy and temperature is depicted in Fig. 11. It is seen from Fig. 11 that activation energies of free-radical reactions (steps 1 and 2) are obviously temperature-dependent, but activation energies of concerted reactions (steps 3–5) show limited temperature-dependency. With the increase of temperature, the activation energies of free-radical reactions (steps 1 and 2) decrease obviously, while the activation energies of concerted reactions (steps 3–5) show little change. Jarvis et al. [36] studied the pyrolysis of PPE as lignin model compound in a wide temperature range of 300–1350 °C to determine the importance of concerted reaction and free-radical reaction pathways, and experimental results indicate that the free-radical reaction (C–O homolysis) is significant at high temperatures (>1000 °C), whereas the concerted reactions are significant at lower temperatures, and the C–C homolysis mechanism is minor at all temperatures. The structure of  $\beta$ -O-4 type lignin dimer model compound **1** is similar to PPE, but more complex than PPE. We can see from Table 1 that at 293 K the activation energy of concerted reaction (step 5) is the lowest, however, with the increase of temperature, the activation energy of free-radical reaction (C–O homolysis) becomes the lowest at 1900 K. Our calculation results indicate that the concerted reactions would dominate over free-radical homolytic reactions at lower temperatures, while at high temperatures the free-radical reaction (C–O homolysis) would dominate over the concerted reactions, which is basically consistent with the result of the literature [36].

#### 4. Conclusions

In this work, the pyrolysis mechanisms of  $\beta$ -O-4 type lignin dimer model compound **1** have been theoretically investigated by employing DFT methods at B3LYP/6-31G(d,p) level. Three possible pyrolytic pathways (the homolytic cleavage of C $\beta$ –O bond, the homolytic cleavage of C $\alpha$ –C $\beta$  bond and the concerted reactions) were proposed and the geometries of reactants, transition states, intermediates and products were fully optimized. The activation energies of each reaction step were calculated and the temperature effect on pyrolysis processes was analyzed. The main conclusions are made as follows:

- (1) The order of magnitude of bond dissociation energies for model compound **1** is as follows: C $\beta$ –O < C $\alpha$ –C $\beta$  < C $\alpha$ –OH < C $\beta$ –C $\gamma$  < C $_{aromatic}$ –C $\alpha$  < C $_{aromatic}$ –O, so the initial step in the thermal decomposition of model compound **1** could be the homolytic cleavage of the C $\beta$ –O bond, and C $\alpha$ –C $\beta$  bond cleavage could be a competitive initial reaction.

- (2) The homolytic cleavage reaction of C $\beta$ –O bond and concerted reaction pathways (3) could be the major reaction channels, and the homolytic cleavage reaction of C $\alpha$ –C $\beta$  bond and concerted reaction pathways (1) and (2) could be the competitive reaction channels in pyrolysis processes.
- (3) The main products of model compound **1** pyrolysis could be phenolic compounds such as phenol **4**, phenyl acetone alcohol **6**, phenyl acrylketone **8**, phenyl propanediol **9** and benzene-propanal **15**, and the main competitive products could be benzaldehyde **11**, phenylcarbinol **19**, phenyl ether such as phenoxy alcohol **20**, phenoxy vinyl alcohol **25** and phenoxy acetaldehyde **28**.
- (4) The concerted reactions would dominate over free-radical homolytic reactions at lower temperatures, while at high temperatures the free-radical reaction (C–O homolysis) would dominate over the concerted reactions.

#### Acknowledgments

This work was supported by the National Natural Science Foundation of China (No. 51266002, 50776101), the Natural Science Research Funds of the Department of Education of Guizhou Province (No. [2013]405), the Open Research Funds of Key Laboratory of Low-grade Energy Utilization Technologies and Systems (Chongqing University), Ministry of Education of China (No. LLEUTS-201303) and the Science and Technology Funds of Guizhou Province (No. [2012]2188).

#### References

- [1] A.V. Bridgwater, D. Meier, D. Radlein, An overview of fast pyrolysis of biomass, *Org. Geochem.* 30 (1999) 1479–1493.
- [2] P. Mckendry, Energy production from biomass (part 1): overview of biomass, *Bioresour. Technol.* 83 (2002) 37–46.
- [3] J. Huang, C. Liu, H. Tong, W. Li, D. Wu, Theoretical studies on pyrolysis mechanism of xylopyranose, *Comput. Theor. Chem.* 1001 (2012) 44–50.
- [4] M. Asmadi, H. Kawamoto, S. Saka, Thermal reactivities of catechols/pyrogallols and cresols/xylenols as lignin pyrolysis intermediates, *J. Anal. Appl. Pyrol.* 92 (2011) 76–87.
- [5] C. Liu, J. Huang, X. Huang, H. Li, Z. Zhang, Theoretical studies on formation mechanisms of CO and CO $_2$  in cellulose pyrolysis, *Comput. Theor. Chem.* 649 (2011) 207–212.
- [6] D.J. Nowakowski, A.V. Bridgwater, D.C. Elliott, D. Meier, P. de Wild, Lignin fast pyrolysis: results from an international collaboration, *J. Anal. Appl. Pyrol.* 88 (2010) 53–72.
- [7] J. Huang, X. Li, D. Wu, H. Tong, W. Li, Theoretical studies on pyrolysis mechanism of guaiacol as lignin model compound, *J. Renew. Sustain. Energy* 5 (2013) 043112.
- [8] N. Mahinpey, P. Murugan, T. Mani, R. Raina, Analysis of bio-oil, biogas, and biochar from pressurized pyrolysis of wheat straw using a tubular reactor, *Energy Fuels* 23 (2009) 2736–2742.
- [9] M.W. Jarvis, Ph.D. thesis, University of Colorado, Boulder, 2008.
- [10] Y.Y. Peng, S.B. Wu, Fast pyrolysis characteristics of sugarcane bagasse hemicellulose, *Cell. Chem. Technol.* 45 (2011) 605–612.
- [11] G. Jiang, D.J. Nowakowski, A.V. Bridgwater, A systematic study of the kinetics of lignin pyrolysis, *Thermochim. Acta* 498 (2010) 61–66.
- [12] B. Iatridis, G.R. Gavalas, Pyrolysis of a precipitated kraft lignin, *Ind. Eng. Chem. Prod. Res. Dev.* 18 (1979) 127–130.
- [13] J.A. Caballero, R. Font, A. Marcilla, Pyrolysis of Kraft lignin: yields and correlations, *J. Anal. Appl. Pyrol.* 39 (1997) 161–183.
- [14] G. Jiang, D.J. Nowakowski, A.V. Bridgwater, Effect of the temperature on the composition of lignin pyrolysis products, *Energy Fuels* 24 (2010) 4470–4475.
- [15] S. Wang, K. Wang, Q. Liu, Y. Gu, Z. Luo, K. Cen, T. Fransson, Comparison of the pyrolysis behavior of lignins from different tree species, *Biotechnol. Adv.* 27 (2009) 562–567.
- [16] Q. Liu, S. Wang, Y. Zheng, Z. Luo, K. Cen, Mechanism study of wood lignin pyrolysis by using TG-FTIR analysis, *J. Anal. Appl. Pyrol.* 82 (2008) 170–177.
- [17] A. Vuori, J.B. Bredenberg, Thermal chemistry pathways of substituted anisoles, *Ind. Eng. Chem. Res.* 26 (1987) 359–365.
- [18] A. Beste, A.C. Buchanan III, Computational study of bond dissociation enthalpies for lignin model compounds. Substituent effects in phenethyl phenyl ethers, *J. Org. Chem.* 74 (2009) 2837–2841.
- [19] A. Beste, A.C. Buchanan III, R.J. Harrison, Computational prediction  $\alpha/\beta$  selectivities in the pyrolysis of oxygen-substituted phenethyl phenyl ethers, *J. Phys. Chem. A* 112 (2008) 4982–4988.
- [20] S. Chu, A.V. Subrahmanyam, G.W. Huber, The pyrolysis chemistry of a  $\beta$ -O-4 type oligomeric lignin model compound, *Green Chem.* 35 (2013) 125–136.

- [21] M. Asmadi, H. Kawamoto, S. Saka, Thermal reactions of guaiacol and syringol as lignin model aromatic nuclei, *J. Anal. Appl. Pyrol.* 92 (2011) 88–98.
- [22] P.F. Britt, A.C. Buchanan III, M.J. Cooney, D.R. Martineau, Flash vacuum pyrolysis of methoxy-substituted lignin model compounds, *J. Org. Chem.* 65 (2000) 1376–1389.
- [23] S. Wang, Y. Liao, H. Tan, Z. Luo, K. Cen, Mechanism of cellulose rapid pyrolysis: II. Mechanism analysis, *J. Fuel Chem. Technol.* 31 (2003) 317–321.
- [24] J.A. Conesa, J.A. Caballero, A. Marcilla, Analysis of different kinetic models in the dynamic pyrolysis of cellulose, *Thermochim. Acta* 254 (1995) 175–192.
- [25] Y.Y. Peng, S.B. Wu, Fast pyrolysis of hemicellulose in wheat straw, *J. Fuel Chem. Technol.* 39 (2011) 21–25.
- [26] H. Wang, H. Yang, X. Ran, Z. Wen, Q. Shi, The pyrolysis mechanism of carbon matrix precursor toluene used as carbon material, *J. Mol. Struct. Theochem.* 518 (2002) 1–9.
- [27] J. Huang, C. Liu, S. Wei, X. Huang, H. Li, Density functional theoretical studies on pyrolysis mechanism of  $\beta$ -D-glucopyranose, *J. Mol. Struct. Theochem.* 958 (2010) 64–70.
- [28] J. Li, K. Yoshizawa, Energetics and mechanism of dinitrogen cleavage at a mononuclear surface Tantalum center: a new way of dinitrogen reduction, *Angew. Chem. Int. Ed.* 47 (2008) 8040–8043.
- [29] J. Li, K. Yoshizawa, Computational evidence for hydrogen generation by reductive cleavage of water and  $\alpha$ -H abstraction on a molybdenum complex, *Angew. Chem. Int. Ed.* 50 (2011) 11972–11975.
- [30] A.D. Becke, Density-functional thermochemistry. III. The role of exact exchange, *J. Chem. Phys.* 98 (1993) 5648–5652.
- [31] C. Lee, W. Yang, R.G. Parr, Development of the Colle–Salvetti correlation-energy formula into a functional of the electron density, *Phys. Rev. B* 37 (1988) 785–789.
- [32] C. Gonzalez, H.B. Schlegel, An improved algorithm for reaction path following, *J. Chem. Phys.* 90 (1989) 2154–2161.
- [33] M.J. Frisch, G.W. Trucks, H.B. Schlegel, et al., Gaussian 03, Gaussian, Inc., Pittsburgh, PA, 2003.
- [34] C. Amen-Chen, H. Pakdel, C. Roy, Production of monomeric phenols by thermochemical conversion of biomass: a review, *Bioresour. Technol.* 79 (2001) 277–299.
- [35] H. Tan, S. Wang, Z. Luo, C. Yu, K. Cen, Experimental study of lignin flash pyrolysis, *J. Zhejiang Univ. (Eng. Sci.)* 39 (2005) 710–714.
- [36] M.W. Jarvis, J.W. Daily, H.H. Carstensen, A.M. Dean, S. Sharma, D.C. Dayton, D.J. Robichaud, M.R. Nimlos, Direct detection of products from the pyrolysis of 2-phenethyl phenyl ether, *J. Phys. Chem. A* 115 (2011) 428–438.